IEEE Photonics Journal
An IEEE Photonics Society Publication

Open Access

Graphene Q-Switched Compact Yb:YAG Laser

Volume 7, Number 5, October 2015

Josep Maria Serres
Venkatesan Jambunathan
Xavier Mateos
Pavel Loiko
Antonio Lucianetti
Tomas Mocek
Konstantin Yumashev
Valentin Petrov
Uwe Griebner
Magdalena Aguiló
Francesc Díaz

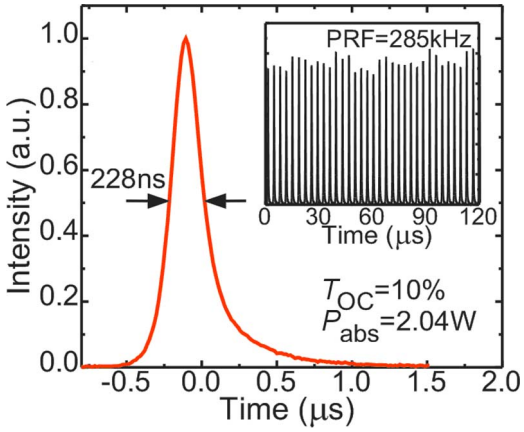

DOI: 10.1109/JPHOT.2015.2476756
1943-0655

IEEE photonics SOCIETY

IEEE

Graphene Q-Switched Compact Yb: YAG Laser

Josep Maria Serres,[1] Venkatesan Jambunathan,[2] Xavier Mateos,[1] Pavel Loiko,[1,3] Antonio Lucianetti,[2] Tomas Mocek,[2] Konstantin Yumashev,[3] Valentin Petrov,[4] Uwe Griebner,[4] Magdalena Aguiló,[1] and Francesc Díaz[1]

[1]Física i Cristal lografia de Materials i Nanomaterials (FiCMA-FiCNA), Universitat Rovira i Virgili, 43007 Tarragona, Spain
[2]HiLASE Centre, Institute of Physics ASCR, 252 41 Dolní Břežany, Czech Republic
[3]Center for Optical Materials and Technologies, Belarusian National Technical University, Minsk 220013, Belarus
[4]Max Born Institute for Nonlinear Optics and Short Pulse Spectroscopy, 12489 Berlin, Germany

DOI: 10.1109/JPHOT.2015.2476756

Manuscript received July 3, 2015; accepted August 20, 2015. Date of publication September 3, 2015; date of current version September 21, 2015. This work was supported by the Spanish Government under Project MAT2011-29255-C02-02, Project MAT2013-47395-C4-4-R, and Project TEC2014-55948-R; by the Generalitat de Catalunya under Project 2014SGR1358; by the European Regional Development Fund, the European Social Fund, and the state budget of the Czech Republic (Project HiLASE: CZ.1.05/2.1.00/01.0027 and Project DPSSLasers: CZ.1.07/2.3.00/20.0143); and by the Czech Science Foundation (GACR) under Project GA14-01660S and Grant RVO 68407700. F. D. acknowledges additional support through the ICREA academia award for excellence in research. Corresponding author: X. Mateos (e-mail: xavier.mateos@urv.cat).

Abstract: We describe a compact Yb:YAG laser Q-switched by a graphene-based saturable absorber and pumped by a laser diode at 932 or 969 nm. The compact laser generates a maximum average output power value of 185 mW at 1032 nm with a slope efficiency value of 12%. The shortest duration of the Q-switched pulse achieved is 228 ns at a repetition frequency of 285 kHz. The maximum pulse energy amounts to 0.65 μJ.

Index Terms: Graphene, saturable absorber, Q-switched laser.

1. Introduction

Graphene is a 2-D material consisting of a single layer of carbon atoms arranged in a honeycomb lattice. It possesses the unique feature of a zero bandgap, as its valence and conduction bands contact in the Dirac point. This determines a characteristic linear absorption with weak wavelength dependence. Despite being composed of one atomic layer, graphene absorbs a remarkable amount of incident light ($\pi\alpha \approx 2.3\%$, determined by the fine structure constant α) [1]. In addition, graphene exhibits saturable absorption [2], which is of practical use for (ultra) short-pulse (passively Q-switched and mode-locked) lasers [3]. The exposure of graphene to low-intensity light results in an excitation of electrons to the conduction band. However, at a certain light intensity, this band becomes completely filled in accordance with the Pauli blocking principle and bleaching occurs. The nonlinear properties of graphene as a saturable absorber (SA) are almost wavelength independent for the 0.8–3 μm spectral range [2]. The modulation depth of graphene-based SAs can be increased with the use of multi-layered structures. Graphene-SAs show high damage threshold, low saturation intensity and ultrafast carrier dynamics [4], [5]. Graphene also stands for its high thermal conductivity [6].

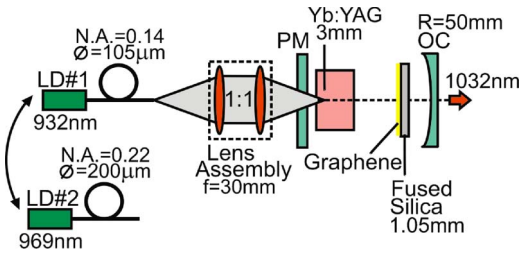

Fig. 1. Scheme of the passively-cooled compact Yb:YAG laser Q-switched by a graphene-SA: LD—laser diode, PM—pump mirror, OC—output coupler.

Ytterbium (Yb^{3+}) doped materials are attractive for laser emission at ~1 μm. The Yb^{3+} ion possesses a simple energy level scheme free of parasitic processes such as excited-state absorption and up-conversion; it is characterized by a low quantum defect (Stokes shift); and, finally, Yb lasers can be conveniently pumped with commercial InGaAs laser diodes. Graphene can be a cost-effective alternative to the typical SAs for Yb lasers such as Cr:YAG [7], semiconductor SA mirrors [8], and GaAs [9].

Passive Q-switching (PQS) of ~1 μm lasers with a graphene-SA has been intensively studied in recent years. There are several reports on graphene PQS of Nd-doped "bulk" lasers, reaching sub-100 ns pulse durations and pulse energies of tens of μJ [10]–[13]. Typically, the increase of the number of graphene layers to ~10 was used to improve the Q-switched performance by varying the modulation depth. PQS of Yb-fiber lasers with graphene SAs was reported in [14]–[16]. Typical values of the average output power were tens of mW and pulse durations were shorter than 100 ns. Spectral tunability of such lasers was demonstrated in [16]. Recently, a lot of activity has been devoted to graphene PQS of Yb waveguide lasers. With an Yb phosphate glass waveguide laser, 140 ns, 27 nJ pulses were extracted at 1057 nm in [17] using graphene deposited on the output coupler (OC). In [18], an Yb:KYW planar waveguide laser was Q-switched by evanescent-field interaction with graphene resulting in 349 ns, 59 nJ pulses. In [19], with an Yb:Y_2O_3 waveguide laser, pulses as short as 98 ns were generated and in [20], the output power of this laser was scaled up to 456 mW. Mode-locking of an Yb laser with graphene was reported in [21] and [22].

We were not aware of any "bulk" Yb-laser Q-switched with graphene which motivated us to study the bulk geometry with an outstanding laser material such as Yb:YAG offering more opportunities for power scaling compared to waveguide lasers. In addition, such a configuration could provide shorter Q-switched pulses and higher energies compared to fiber or waveguide lasers. Here we report on PQS of a compact Yb:YAG laser by using a commercial single-layer graphene SA. The effect of the pump wavelength at 932 and 969 nm on the laser performance is also studied.

2. Experimental

The commercial 3 at.% Yb:YAG crystal was 3 mm thick with a diameter of 10 mm. Both surfaces were polished to laser quality and antireflection (AR) coated for 0.9–1.1 μm. The crystal was mounted in a copper holder without any active cooling for a compact set-up and placed in a plano-concave laser cavity. The latter was composed of a flat pump mirror (PM) AR-coated for 0.9–0.97 μm and high-reflection (HR) coated for 1.0–1.1 μm, and a concave output coupler (OC), see Fig. 1. Two OCs with transmittance $T_{OC} = 5\%$ and 10% at 1.0–1.1 μm were tested. A commercial transmission-type graphene SA (Graphene Supermarket) was inserted at normal incidence between the crystal and the OC. The SA consisted of a 1.05 mm-thick fused silica substrate with a single-layer graphene deposited by chemical vapor deposition (CVD) method. The clean face of the substrate was uncoated. The air gaps between PM, Yb:YAG crystal, SA and OC were below 0.5 mm thus resulting in a total geometrical cavity length of ~6 mm. The reduction of the cavity length and consequently the cavity round trip time enables the generation of shorter Q-switched pulses.

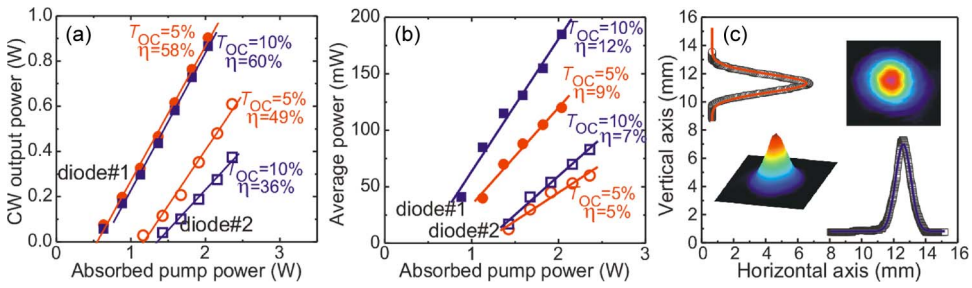

Fig. 2. Input-output characteristics of the compact Yb:YAG laser pumped by diode #1 and diode #2 in the CW (a) and passively Q-switched (b) operation modes; symbols denote the experimental data, lines correspond to fits for the slope (η) calculation; (c) typical beam profile of the compact Q-switched Yb:YAG laser (diode #1, $P_{abs} = 2$ W, $T_{OC} = 10\%$).

Two fiber-coupled InGaAs laser diodes were used to pump the Yb:YAG crystal. These two diodes provided two different mode-matching conditions for the pump and laser modes. The first diode (#1) operated at 932 nm and the emission of the second diode (#2) was stabilized at 969 nm by a volume Bragg grating (VBG). The output of the diodes was reimaged into the crystal by a lens assembly with a ratio of 1 : 1 (focal length: 30 mm). Thus, the pump spot radii in the crystal were ~52 μm and ~100 μm for diode #1 and #2, respectively. The single-pass absorption in the Yb:YAG crystal was measured to be 33% (diode #1) and 46% (diode #2). As the OCs provided a partial reflection at the pump wavelength, the Yb:YAG crystal was pumped in a two-ass scheme. The calculated overall absorption amounted to 42% (diode #1) and 55% (diode #2). No bleaching of the crystal absorption was detected.

A fast InGaAs photodiode (rise time: 200 ps) and a 2 GHz digital oscilloscope were used for detection of the Q-switched pulses. The output beam profile was measured with a FLIR SC7210 thermal imaging camera.

3. Results and Discussion

First, we studied the output performance of the compact Yb:YAG laser in the continuous-wave (CW) regime; see Fig. 2(a). When pumping with diode #1, a maximum output power of 0.9 W was achieved with a slope efficiency $\eta = 58\%$ (for $T_{OC} = 5\%$). The laser threshold was ~0.5 W. A very similar performance was observed for $T_{OC} = 10\%$, with a slightly higher slope of $\eta = 60\%$. For diode #2, the laser performance was inferior, mainly related to the 4 times larger pump spot. For $T_{OC} = 5\%$ and approximately the same pump level as for diode #1, only 0.6 W of CW output was extracted with a reduced slope efficiency $\eta = 49\%$, as well as an increased threshold, ~1.1 W. For $T_{OC} = 10\%$, the laser performance was even worse: the threshold was even higher but also the slope efficiency η dropped to 36%, probably due to imperfect alignment.

Stable Q-switching of the compact Yb:YAG laser was achieved for diodes #1 and #2 and both OCs studied; no damage of the graphene-SA was observed. The corresponding input-output dependences in Fig. 2(a) and (b) are all linear thus showing no negative impact of thermal effects. The laser wavelength λ_l was in all cases 1032 nm and the output mode circular and close to TEM_{00} ($M^2_{x,y} < 1.1$), a typical profile is shown in Fig. 2(c). As in the case of CW lasing, better laser performance was observed when pumping with diode #1. For $T_{OC} = 10\%$, the maximum average output power was 185 mW corresponding to the highest slope of $\eta = 12\%$ and a CW to PQS efficiency of 21%. The laser threshold was only slightly increased with respect to the CW regime, amounting to ~0.6 W. For $T_{OC} = 5\%$, we extracted 120 mW with $\eta = 9\%$. When pumping with diode #2, the maximum average output power and slope efficiency amounted to 83 mW and $\eta = 7\%$ ($T_{OC} = 10\%$), and 60 mW and $\eta = 5\%$ ($T_{OC} = 10\%$). For diode #2, laser thresholds were as high as ~1.3 W. Table 1 summarizes the output characteristics of the compact passively Q-switched Yb:YAG laser.

The unchanged laser wavelength after insertion of the SA, as well as the moderate increase of the threshold indicate that the losses introduced by the graphene SA are relatively low

TABLE 1

Output characteristics* of the compact graphene Q-switched Yb:YAG laser

Pump	T_{OC}	P_{th}, W	P_{out}, mW	η, %	η_{conv}, %	t_p, ns	PRF, kHz	E_{out}, μJ	P_{peak}, W
diode #1	5%	0.88	120	9	13	270	240	0.50	1.9
	10%	0.6	185	12	21	228	285	0.65	2.9
diode #2	5%	1.35	60	5	10	303	269	0.22	0.7
	10%	1.25	83	7	21	323	202	0.41	1.3

*P_{th} – laser threshold; P_{out} – average output power; η – slope efficiency; t_p – pulse duration; η_{conv} – CW to PQS conversion efficiency; PRF – pulse repetition frequency; E_{out} – pulse energy; P_{peak} – peak power.

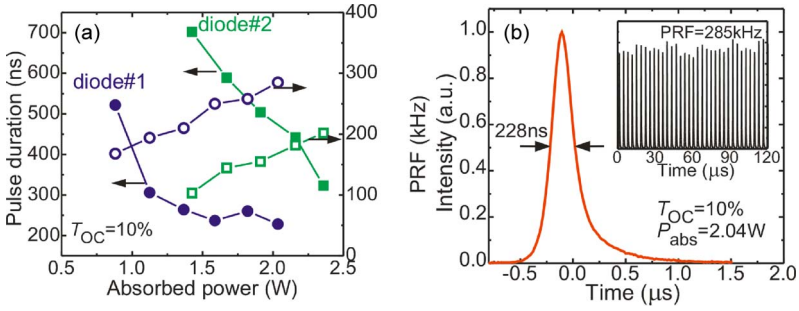

Fig. 3. (a) Pulse duration and pulse repetition frequency (PRF) versus absorbed pump power of the compact graphene Q-switched Yb:YAG laser. (b) Oscilloscope trace of the shortest Q-switched pulse obtained; inset corresponding pulse train.

(compared to the other cavity losses including reabsorption losses [23]). However, the substantial reduction of the slope efficiency in the Q-switching regime indicates that these losses are higher than the output coupling losses. Indeed, in addition to the 4.6% double-pass low-signal absorption loss one calculates ~13% double-pass reflection losses due to the uncoated fused silica substrate.

Q-switching instabilities for $P_{abs} > 2$ W (diode #1) and > 2.4 W (diode #2) are attributed to heating of the graphene SA due to residual (non-absorbed) pump [24].

The highest Q-switched output power (diode #1, $T_{OC} = 10\%$) also corresponded to the generation of the shortest pulses, whose duration ranged from 522 to 228 ns with P_{abs} increasing from 0.9 to 2.04 W, see Fig. 3(a). Saturation was observed for the pulse shortening. The corresponding pulse repetition frequency (PRF) was found to depend near-linearly on the pump level, ranging from 168 to 285 kHz. The oscilloscope trace of the shortest Q-switched pulse achieved and the corresponding pulse train are shown in Fig. 3(b). The intensity fluctuations in the pulse train are < 10%. When pumping with diode #2 and again using $T_{OC} = 10\%$, the shortest pulse duration was 323 ns at a PRF of 202 kHz. The pulse durations and PRFs for the 5% OC are included in Table 1.

Based on the average output power, PRF and pulse duration, we calculated pulse energies and peak powers, see Fig. 4 and Table 1. The maximum values are pulse energy of 0.65 μJ (diode #1) and 0.41 μJ (diode #2) and peak power of 2.9 W (diode #1) and 1.3 W (diode #2).

The thermal conditions are different for the two pump diodes used due to the different pump spot radii w_p (~52 and 100 μm) and wavelengths λ_p (932 and 969 nm). The latter also indicates different fractional heat load η_h that can be estimated for Yb^{3+} ions as Stokes shift $1 - \lambda_p/\lambda_l$ [25], giving $\eta_h = 0.097$ for diode #1 and only 0.061 for diode #2. The parameters of the thermal lens in the crystal depend on both the w_p and η_h values. However, the typical thermal lens effect of roll-over of the output power dependence is not evident in our case, see Fig. 2.

Another important factor affecting the laser efficiency is the mode-matching condition for pump and laser modes. To analyze mode-matching, we determined the sensitivity factor of the

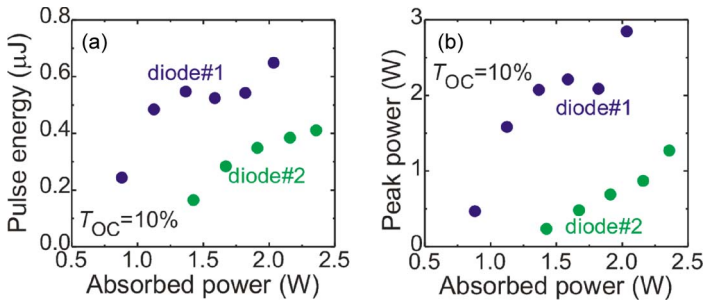

Fig. 4. (a) Pulse energies and (b) peak powers for the compact Yb:YAG laser passively Q-switched by a graphene-SA.

TABLE 2

Mode-matching analysis* for the compact Yb:YAG laser

Pump	λ_p, nm	η_h	w_p, μm	M, $m^{-1}W^{-1}$	w_l, μm
diode #1	932	0.097	52±5	10.0 (r), 9.2 (θ)	57±5
diode #2	969	0.061	100±5	1.82 (r), 1.69 (θ)	63±5

*w_p (w_l) - radius of the pump (laser) mode; η_h – fractional heat load; λ_p – pump wavelength; M – sensitivity factors of the thermal lens

thermal lens in the Yb:YAG crystal when pumping with the two diodes. It is defined as $M_{r(\theta)} = dD/dP_{abs}$ where D is the optical (refractive) power of the lens and P_{abs} is the absorbed pump power; $r(\theta)$ correspond to the orthogonal meridional planes of the thermal lens [25], [26].

The sensitivity factor of the thermal lens in Yb:YAG pumped with diode #1 is $M_{r(\theta)} = 10.0$ and 9.2 m^{-1}/W. For diode #2, as expected, it is ~5 times lower, $M_{r(\theta)} = 1.82$ and 1.69 m^{-1}/W. As determined from ABCD modeling of the "hot" laser cavity with internal thermal lens, the laser mode radius in the crystal is $w_l = 57 \pm 5$ μm for diode #1 resulting in a good mode-matching ($w_p = 52$ μm). For diode #2, w_l is 63 ± 5 μm, which is substantially lower than the pump mode radius ($w_p \sim 100$ μm) thus leading to worse mode-matching. The latter explains the deterioration of the laser performance of the compact Yb:YAG laser when pumped by diode #2 as compared to diode #1, see Fig. 2. Table 2 summarizes the mode-matching analysis. In addition, a smaller size of the laser mode on the SA is expected for diode #1.

As can be deduced from Table 2, the astigmatism of the thermal lens, defined as $S = \Delta M/M$ [27], equals ~8%. Such a small value is inherent to cubic crystals [25] and is responsible for the high quality of the spatial profile of the output laser beam of the Yb:YAG laser.

The stronger bleaching of the SA due to the higher intracavity fluence accounts for the observed shorter pulses. Indeed, the intracavity intensity on the SA reaches 0.57 MW/cm^2 for diode #1 ($P_{abs} = 2.04$ W). This is close to the saturation intensity of single layer graphene: $I_{sat} = 0.5 - 0.7$ MW/cm^2 [2], [28], [29]; thus, the graphene SA is almost bleached. This agrees with the saturation of the pulse duration vs. pump power dependence in Fig. 3(a). For diode #2 ($P_{abs} = 2.4$ W), the intracavity intensity is ~0.2 MW/cm^2, and the pulses are longer.

It should be noted that although the linear absorption of graphene is wavelength-insensitive due to its near zero bandgap structure, its nonlinear properties show dispersion. In particular, I_{sat} is higher at shorter wavelength [29]. To understand this, one should consider in more detail the mechanism of bleaching of graphene. For low intensity incident light (with a corresponding photon energy hv), electrons in the valence band having energy of $E_F - hv/2$ can be excited to the conduction band with energy of $E_F + hv/2$ (E_F is the Fermi energy). When all electrons with energies from $E_F - hv/2$ to E_F are excited, the corresponding region of the conduction band is full and further excitation is prevented by the Pauli blocking principle; therefore, bleaching occurs. Thus, for ns pulses, the saturation intensity of graphene is proportional to the number of

electrons in the valence band with energy ranging from $E_F - h\nu/2$ to E_F. In other words, I_{sat} should increase with $h\nu$. Thus, it is, in principle, more difficult to achieve complete saturation in Q-switched Yb-lasers as compared with previously studied Tm or Ho lasers.

Previous schemes for graphene PQS of Yb lasers based on fiber or waveguide configurations with strong mode confinement avoided this problem [14]–[20]. However, for a bulk laser, the proper design of the laser cavity providing high intracavity fluence is crucial for the achievement of short pulses and stable PQS. In the present paper, this problem was solved through the implementation of a compact laser. A problem when employing a SA in a short cavity is typically its heating due to a residual non-absorbed pump that can be overcome with the use of higher crystal doping. Although the transmission of a single layer graphene-SA at the pump wavelength is rather high $(T > 96\%)$, its implementation in a quasi-three-level Yb laser faces a relatively high threshold. This shows the increased difficulty of graphene-SA PQS of Yb lasers, as compared with their Nd counterparts.

Further pulse shortening in the studied compact laser can be achieved with a multi-layer graphene. Considering the nonlinear properties of the multi-layer graphene we estimate that the optimum number of layers n is 2–3. In this case, the modulation depth of the SA will increase near proportionally to the number of layers and I_{sat} will be even slightly lower. For $n \sim 7$–9, a fast increase of the non-saturable loss due to enhanced scattering is expected [2], [29]. On the other hand, in the present work with a single-layer graphene the Q-switching conversion efficiency is modest $(\eta_{conv} = 21\%)$ presumably due to high insertion losses of the graphene SA and this effect shall be taken into account, too. In addition, as it can be seen in Fig. 3(b), the pulse profile is not symmetric, exhibiting a slow trailing edge, which is an indication of less than optimum output coupling.

As an additional remark, we investigated Q-switching of the Yb:YAG laser also using a hemispherical cavity with the SA placed between the laser crystal and OC. Although this attempt failed (only unstable operation), CW laser operation was very efficient ($\eta = 65\%$ with diode #1 and $T_{OC} = 5\%$). From ABCD modeling of such a cavity, we determined a radius of the laser mode on the SA nearly 2 times higher than that of the compact laser preventing proper bleaching of the graphene.

4. Conclusion

We report on the first realization of PQS of an ytterbium bulk laser with graphene as SA. We used Yb:YAG as a gain medium and commercial single-layer graphene on a silica substrate as SA. Mode-matching affects significantly the laser performance. Pulses as short as 228 ns with a maximum pulse energy of 0.65 μJ are extracted. Further shortening of the pulse duration is expected by increasing the number of graphene layers in the SA to profit from the resulting higher modulation depth. The thermal lens properties of the Yb:YAG crystal also contribute to the excellent spatial quality of the laser beam with $M^2_{x,y} < 1.1$.

References

[1] R. R. Nair *et al.*, "Fine structure constant defines visual transparency of graphene," *Science*, vol. 320, no. 5881, p. 1308, Jun. 2008.
[2] Q. L. Bao *et al.*, "Atomic-layer graphene as a saturable absorber for ultrafast pulsed lasers," *Adv. Funct. Mater.*, vol. 19, no. 19, pp. 3077–3083, Oct. 2009.
[3] Z. Sun *et al.*, "Graphene mode-locked ultrafast laser," *ACS Nano*, vol. 4, no. 2, pp. 803–810, Feb. 2010.
[4] J. M. Dawlaty, S. Shivaraman, M. Chandrashekhar, F. Rana, and M. G. Spencer, "Measurement of ultrafast carrier dynamics in epitaxial graphene," *Appl. Phys. Lett.*, vol. 92, no. 4, Jan. 2008, Art. ID. 042116.
[5] G. Xing, H. Guo, X. Zhang, T. C. Sum, and C. H. A. Huan, "The physics of ultrafast saturable absorption in graphene," *Opt. Exp.*, vol. 18, no. 5, pp. 4184–4197, Mar. 2010.
[6] A. A. Balandin *et al.*, "Superior thermal conductivity of single-layer graphene," *Nano Lett.*, vol. 8, no. 3, pp. 902–907, Mar. 2008.
[7] J. Dong, A. Shirakawa, and K. I. Ueda, "Sub-nanosecond passively Q-switched Yb:YAG/Cr^{4+}:YAG sandwiched microchip laser," *Appl. Phys. B*, vol. 85, no. 4, pp. 513–518, Dec. 2006.
[8] G. J. Spuhler *et al.*, "A passively Q-switched Yb:YAG microchip laser," *Appl. Phys. B*, vol. 72, no. 3, pp. 285–287, Jan. 2001.

[9] Q. Liu *et al.*, "GaAs as a passive Q-switch and Brewster plate for pulsed Yb:YAG laser," *Opt. Commun.*, vol. 222, no. 1–6, pp. 355–361, Jul. 2003.
[10] H. H. Yu *et al.*, "Large energy pulse generation modulated by graphene epitaxially grown on silicon carbide," *ACS Nano*, vol. 4, no. 12, pp. 7582–7586, Dec. 2010.
[11] H. Yu *et al.*, "Graphene as a Q-switcher for neodymium-doped lutetium vanadate laser," *Appl. Phys. Exp.*, vol. 4, no. 2, Feb. 2011, Art. ID. 022704.
[12] Y. Zhao *et al.*, "Dual-wavelength synchronously Q-switched solid-state laser with multi-layered graphene as saturable absorber," *Opt. Exp.*, vol. 21, no. 3, pp. 3516–3522, Feb. 2013.
[13] X. Li, J. Xu, Y. Wu, J. He, and X. Hao, "Large energy laser pulses with high repetition rate by graphene Q-switched solid-state laser," *Opt. Exp.*, vol. 19, no. 10, pp. 9950–9955, May 2011.
[14] J. Liu, S. Wu, Q.-H. Yang, and P. Wang, "Stable nanosecond pulse generation from a graphene-based passively Q-switched Yb-doped fiber laser," *Opt. Lett.*, vol. 36, no. 20, pp. 4008–4010, Oct. 2011.
[15] L. Zhang *et al.*, "Graphene incorporated Q-switching of a polarization maintaining Yb-doped fiber laser," *Laser Phys. Lett.*, vol. 9, no. 12, pp. 888–892, Oct. 2012.
[16] L. Zhang *et al.*, "Wavelength tunable passively Q-switched Yb-doped double-clad fiber laser with graphene grown on SiC," *Chin. Opt. Lett.*, vol. 12, no. 2, Feb. 2014, Art. ID. 021405.
[17] A. Choudhary, S. Dhingra, B. D'Urso, P. Kannan, and D. P. Shepherd, "Graphene Q-switched mode-locked and Q-switched ion-exchanged waveguide lasers," *IEEE Photon. Technol. Lett.*, vol. 27, no. 6, pp. 646–649, Mar. 2015.
[18] J. W. Kim *et al.*, "Graphene Q-switched Yb:KYW planar waveguide laser," *AIP Adv.*, vol. 5, no. 1, Jan. 2015, Art. ID. 017110.
[19] A. Choudhary *et al.*, "Q-switched operation of a pulsed-laser-deposited Yb:Y_2O_3 waveguide using graphene as a saturable absorber," *Opt. Lett.*, vol. 39, no. 15, pp. 4325–4328, Aug. 2014.
[20] A. Choudhary *et al.*, "456-mW graphene Q-switched Yb:yttria waveguide laser by evanescent-field interaction," *Opt. Lett.*, vol. 40, no. 9, pp. 1912–1915, May 2015.
[21] W. Cai *et al.*, "Graphene saturable absorber for diode pumped Yb:Sc2SiO5 mode-locked laser," *Opt. Laser Technol.*, vol. 65, pp. 1–4, Jan. 2015.
[22] E. Ugolotti *et al.*, "Graphene mode-locked femtosecond Yb:KLuW laser," *Appl. Phys. Lett.*, vol. 101, no. 16, Oct. 2012, Art. ID. 161112.
[23] U. Griebner *et al.*, "Graphene saturable absorber Q-switched Tm:$KLu(WO_4)_2$ laser emitting at 2 μm," presented at the Advanced Solid-State Lasers Conf., Shanghai, China, 2014, Paper ATh2A.16.
[24] J. M. Serres *et al.*, "Tm:$KLu(WO_4)_2$ microchip laser Q-switched by a graphene-based saturable absorber," *Opt. Exp.*, vol. 23, no. 11, pp. 14 108–14 113, Jun. 2015.
[25] S. Chenais, F. Druon, S. Forget, F. Balembois, and P. Georges, "On thermal effects in solid-state lasers: The case of ytterbium-doped materials," *Progr. Quantum Electron.*, vol. 30, no. 4, pp. 89–153, 2006.
[26] P. A. Loiko *et al.*, "Anisotropy of the photo-elastic effect in Nd:KGd(WO4)2 laser crystals," *Laser Phys. Lett.*, vol. 11, no. 5, Mar. 2014, Art. ID. 055002.
[27] P. Loiko, F. Druon, P. Georges, B. Viana, and K. Yumashev, "Thermo-optic characterization of Yb:$CaGdAlO_4$ laser crystal," *Opt. Mater. Exp.*, vol. 4, no. 11, pp. 2241–2249, Nov. 2014.
[28] Q. Bao *et al.*, "Monolayer graphene as a saturable absorber in a mode-locked laser," *Nano Res.*, vol. 4, no. 3, pp. 297–307, Mar. 2011.
[29] F. Zhang, S. Han, Y. Liu, Z. Wang, and X. Xu, "Dependence of the saturable absorption of graphene upon excitation photon energy," *Appl. Phys. Lett.*, vol. 106, no. 9, Mar. 2015, Art. ID. 091102.